RSC Advances

ROYAL SOCIETY OF CHEMISTRY

www.rsc.org/advances

RSCAdvances

ARTICLE

Preparation and properties of polystyrene nanocomposites containing dumbbell-shaped molecular nanoparticles based on polyhedral oligomeric silsesquioxane and [60]fullerene

Received 00th January 20xx,
Accepted 00th January 20xx

DOI: 10.1039/x0xx00000x

www.rsc.org/

Di Han,[a]Qing–Yun Guo,[b] Wen-Bin Zhang,[b]Liu-Xu Liu,[a]and Qiang Fu*[a]

In this study, we first synthesised dumbbell-shaped Janusmolecular nanoparticle (MNP) based on polyhedral oligomeric silsesquioxane (POSS) and [60]fullerene (C_{60}) (POSS-C_{60}) via Bingel-Hirsch cyclopropanation, with the goal of combining their unique physical and chemical characteristics. The successful preparation of this new Janus POSS-C_{60} was confirmed by NMR, FT-IR and MALDI-TOF MS experiments. Then co-precipitation method was used to prepare four kinds of polystyrene(PS)nanocomposites, namely, PS/POSS, PS/C_{60}, PS/POSS/C_{60} (which is a physical mixtureof PS, POSS and C_{60}) and PS/POSS-C_{60}. The effectof POSS, C_{60}, POSS/C_{60} and POSS-C_{60}on the properties of PS was investigated. SEM result suggests a good and similar dispersion for all of the four prepared PS nanocomposites. The glass transition temperature (T_g) of PS is decreased as increasing the filler content in asimilar way for the four kinds of PS nanocpomposites. Rheological result suggests a similar trend of the storage modulus change as increasing of filler content, disregarding the chemical structure of fillers and combination of fillers. However, it was interesting to find that POSS alone is good for mechanical property reinforcement and C_{60}alone is good for thermal stability reinforcement for PS, while POSS-C_{60}, which is a particle with chemically bonded POSS and C_{60}, exhibit better reinforcement of both mechanical propertyand thermal stability compared with pristine POSS, C_{60} and POSS/C_{60}. Our work provides some new idea for the preparation of polymer nanocomposites with novel particle shape and unique properties.

1. Introduction

Polymer nanomaterials are attracting widespread attention during the past decades.[1-8] Blending nanoparticles with polymer is a simple and effective way to prepare functional polymer materials. Among various nanoparticles, polyhedral oligomeric silsesquioxane (POSS) is well-defined organic/inorganic, cube-shaped, perhaps the smallest silica nanoparticle.[6] The diagonal length of POSS cage is around 1 nm, but the molecular size of POSS is tunable with varying R group (a hydrogen atom or an organic functional group).[6, 9] In the past two decades, numerous studies focus on POSS related polymer materials.[6, 10-12] Another nanoparticle, [60]fullerene (C_{60}), a carbon allotrope with a spherical shape composed of 60 carbon atoms，is the most abundant representative of the fullerene family.[13] By resistive heating of graphite, macroscopic quantities of fullerenes were first produced in 1990.[14] Due to the fact that C_{60} has excellent electrical, optical, magnetic and biological properties, an extraordinary outburst of academic and industrial research has been generated on C_{60}.[15, 16]

Using POSS in nanocomposites is a promising issue for design of materials with high performance such as flame resistant nanocomposites,[17] low-dielectric applications,[18] organic solar cells,[19] superhydrophobic materials,[20-22] optical limiting[23] and dental implants,[24] etc. C_{60}, a strong electron acceptor, has found some applications, including photovoltaics.[8, 25, 26] And it was also reported that C_{60} has excellent free-radical-trapping properties and it could reduce the flammability of polymer nanocomposites.[27-30]

On the other hand, POSS and C_{60} are typical “nanoatom” to build molecular nanoparticles (MNP) precisely.[31] Recently, Clarke et al. reported that POSS could be bound either with fulleropyrrolidines[32] or iminofullerene.[33] Cheng et al. presented a lot of wonderful work using MNP based on POSS and C_{60} to build “giant molecules” and studied their self-assembly behaviours.[31, 34-36]Yang et al.[37] reported that POSS link C_{60} dyads with flexible spacer. This kind of MNP also can be seen as Janus particles[38, 39] because POSS and C_{60} have different chemical, physical properties. It is interesting to apply the Janus particles in bending polymer system, especially for the immiscible polymer blends. It has been reported by some researches.[40-42] And this kind of MNP with unique structure may possess fascinating physical and chemical properties. When POSS was grafted on C_{60}, bi-layered structure formed in the solid state of and POSS-C_{60} may have potential applications such as nano-capacitors.[34] Cheng et al. also investigated the

[a] College of Polymer Science & Engineering, State Key Laboratory of Polymer Materials Engineering, Sichuan University, Chengdu 610065,P. R. China
[b] Key Laboratory of Polymer Chemistry & Physics of Ministry of Education, Center for Soft Matter Science and Engineering, College of Chemistry and Molecular Engineering, Peking University, Beijing 100871, P. R. China
*Corresponding author, Qiang Fu, Fax: 0086-28-85405402, Email: qiangfu@scu.edu.cn

photophysical properties of POSS-C_{60}, and the results indicated that POSS-C_{60} is a potentially good electron acceptor for inverted bulk heterojunction polymer solar cells.[43]

Since a lot of work has been done on the property enhancement of polymer matrix by using either POSS nanoparticle or C_{60} nanoparticle, it is logical to ask if MNP based on POSS and C_{60} can be also used as a new nanoparticle for the property enhancement of polymer matrix. What can be expected or if the synergistic effect exist as POSS-C_{60} is used as nanofiller. Nevertheless, this kind of work is seldom found in literature. We do not know if these dumbbell-shaped POSS-C_{60} could be well dispersed in polymer matrix and how they would affect polymer properties.

Herein, we report our efforts on the synthesis of this new kind of nanoparticle and the exploration of its application in polymer reinforcement. To do this, we first covalently linked POSS and C_{60} to obtain a dumbbell-shaped Janus POSS-C_{60}. As depict in **Scheme 1**, ethyl *N*-malonamatepropyllsobutyl-POSS (BPOSS-MAL) **(3)** was first prepared by condensation of aminopropyllsobutyl-POSS (BPOSS-NH_2) **(1)** with ethyl hydrogen malonate. POSS-C_{60} was prepared using **(3)** and C_{60} via Bingel-Hirsch cyclopropanation under mild reaction conditions (I_2, DBU, RT).[44, 45] The synthesis is simple and could be easily scaled-up to obtain mono-adducts of POSS-C_{60}. Then commercially available PS was used as the polymer matrix. We investigated the filler effects of POSS-C_{60}, POSS, C_{60}, and POSS/C_{60} on the properties of PS. From a series of experimental results, it was found that the effect of POSS-C_{60}on PS properties is obviously different with pristine POSS, C_{60} and POSS/C_{60} and using chemical bond connect POSS and C_{60} (POSS-C_{60}) could exhibit a synergestic effect on the mechanical properties and thermal stability of PS nanocomposites.

2. Experimental Section

2.1 Materials

The following chemicals were used as received: BPOSS-NH_2 (Hybrid Plastics, AM0265), [60]fullerene (Yurui (Shanghai) chemical Co., Ltd), ethyl hydrogen malonate (J&K Chemicals, 98%), 4-(dimethylamino)-pyridine (DMAP, J&K Chemicals, 99%), N,N'-diisopropylcarbodiimide (DIPC, J&K Chemicals, 99%), 1,8-diazabicyclo[5.4.0]undec-7-ene (DBU, J&K Chemicals, 98%), iodine (I_2, J&K Chemicals, 98%), $CDCl_3$ (99.8%D, J&K Chemicals, 99.5%). Petroleum ether (PE, 95%, b.p 60-90 °C), ethyl acetate (EA, 99.9%), dichloromethane (DCM, 99.5%) and toluene (99.5%) were purchased from Beijing Tongguang Industry of Fine Chemicals Company. Toluene was dried over CaH_2 and distilled prior to use. Amorphous polystyrene （PS， PG33, 1.04 g/cm^3） was purchased from Sino-foreign Joint Venture Zhenjiang Qimei Chemical Co., Ltd.

2.2 Synthetic procedures.

2.2.1 Synthesis of ethyl N-malonamatepropyllsobutyl-POSS（BPOSS-MAL）. To a CH_2Cl_2 solution (50 mL) of BPOSS-NH_2 (17.49 g, 20 mmol), ethyl hydrogen malonate (3.17 g, 24 mmol), 4-(dimethylamino)-pyridine (DMAP, 0.49 g, 4mmol), *N*,*N*'-diisopropylcarbodiimide (DIPC, 3.79 g, 30 mmol) were added at room temperature. The mixture was stirred at room temperature for 24 h. After that, the solution was filtered by celite and then concentrated to give crude product. After column chromatography with silica gel using petroleum ether/ethyl acetate (v/v = 6/1) as eluent, BPOSS-MAL was obtained as a white powder (18.51 g). Yield: 94%. ^{1}H NMR (400 MHz,$CDCl_3$, 25 ^{o}C) (**Figure 1 a**): δ7.08(br, H, -$CH_2NHCOCH_2$-), 4.14(q, J = 7.1 Hz, 2H, -$CO_2CH_2CH_3$), 3.23(s, 2H, -$COCH_2CO_2$-), 3.20(t, J = 7.1 Hz, 2H, -CH_2CH_2NH-), 1.86 – 1.72(m, 7H, -$CH_2CH(CH_3)_2$), 1.59 – 1.50(m, 2H, -CH_2CH_2CHNH-), 1.23(t, J = 7.1 Hz, 3H, -$CO_2CH_2CH_3$), 0.99(d, J = 6.7 Hz, 42H, -$CH_2CH(CH_3)_2$), 0.53(dd, J = 7.1 Hz, 2.8Hz, 16H, -$SiCH_2CH$-, -$SiCH_2CH_2$-).^{13}C NMR (400 MHz, $CDCl_3$, **Figure S1**): δ (ppm) 169.8, 164.8, 61.5, 41.9, 41.1, 25.7, 23.9, 22.9, 22.5, 14.1, 9.46. FT-IR (KBr, **Figure S2**) ν (cm^{-1}): 3435 (N-H), 1741 (C=O), 1234 (Si-C), 1107 (Si-O). MALDI-TOF MS (**Figure 2a**): calcd monoisotopic mass for $C_{36}H_{77}NNaO_{15}Si_8$ = 1010.33 Da; found: m/z 1010.35 Da (MNa^+).

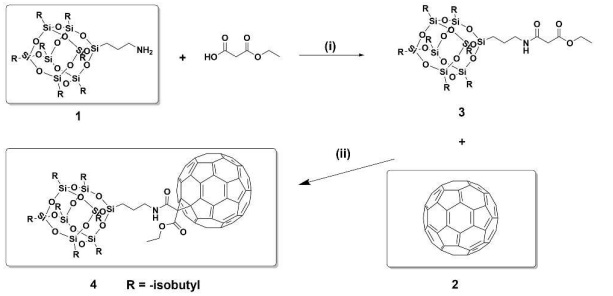

Scheme 1. Chemical structures of BPOSS-NH_2**(1)**, C_{60}**(2)**, the synthetic route to BPOSS-MAL**(3)** and POSS-C_{60}**(4)**. Reaction conditions: i) CH_2Cl_2, DIPC, DMAP, RT (94%); ii) toluene, DBU, I_2, RT (24%)

2.2.2 Synthesis of POSS-C_{60}. An anhydrous toluene solution (600 mL) of **(3)** (1.37g, 1.39 mmol), C_{60} (1.00 g, 1.39 mmol), iodine (1.06g, 4.17 mmol) was added into a 1L round-bottomed flask and stirred for 3 h under nitrogen atmosphere. Then **(3)**, 8-diazabicyclo[5.4.0]undec-7-ene (DBU, 1.06 g, 6.95 mmol) was added and the resulting solution was left stirred at room temperature for 12 h. After that, the reaction mixture was washed with water three times and saturated sodium sulfate solution (100 mL). Then the organic phase was washed with water (100 mL) and brine (50 mL). The organic phase was dried over anhydrous Na_2SO_4 followed by rotary evaporation of the solvent. The crude product was purified by eluting with petroleum ether/toluene (v/v = 1/1) to give (4), as a dark solid (569 mg). Yield: 24%. ^{1}H NMR (400 MHz,$CDCl_3$, 25 ^{o}C) (**Figure 1 b**): δ6.74(t, J = 5.9 Hz, H, -$CH_2NHCOCH_2$-), 4.56(q, J = 7.1 Hz,2H, -$CO_2CH_2CH_3$), 3.56(q, J = 6.5 Hz, 2H, -CH_2CH_2NH-), 1.93 – 1.73(m, 9H, -$CH_2CH(CH_3)_2$, -CH_2CH_2CHNH-), 1.48(t, J = 7.1 Hz, 3H, -$CO_2CH_2CH_3$), 0.95(d, J = 6.7 Hz, 42H, -$CH_2CH(CH_3)_2$), 0.75 – 0.67(m, 4H, -$SiCH_2CH_2$-), 0.60(dd, J = 7.1 Hz, 1.4Hz, 16H, -$SiCH_2CH$-). ^{13}C NMR (400 MHz, $CDCl_3$, **Figure S1**): δ (ppm) 164.7, 161.1, 138.4-145.7, 72.9, 63.7, 56.1, 43.1, 25.7, 23.9, 22.9, 22.5, 14.4, 9.5. FT-IR (KBr, **Figure S2**) ν (cm^{-1}): 3427 (N-H), 1731 (C=O), 1234 (Si-C), 1107 (Si-O), 526 (C-C in C_{60}). MALDI-TOF MS (**Figure 2b**): calcd monoisotopic mass for $C_{96}H_{75}NNaO_{15}Si_8$ = 1728.32 Da; found: m/z 1728.42Da (MNa^+).

2.3 PS nanocomposites preparation.

From now on, POSS was used to instead of BPOSS-NH_2. The PS/POSS, PS/C_{60}, PS/POSS/C_{60} and PS/POSS-C_{60}nanocomposites were prepared by a solution blend and coagulation method with the addition of 0.5, 1, 3, 5 wt% of POSS, C_{60}, POSS/C_{60} and POSS-C_{60}. For brevity, PS/POSS-0.5 means PS/POSS nanocomposites have 0.5% wt%, and others were named in the same way (PS/POSS-1, PS/POSS-3, PS/POSS-5), respectively. It should be noted that there are equimolar POSS and C_{60} in POSS-C_{60} thus for comparison the physical blends (POSS/C_{60}) takes 1:1 molar ratio of POSS andC_{60}. All of the nanocomposites were prepared according to the following general process. Firstly, appropriate amounts of nanoparticles and PS (2 g) were dissolved separately in xylene (50 mL). Secondly, the PS solution and the nanoparticle solution were mixed together and stirred for 6 h. Thirdly, the solution mixture was precipitated into a large amount of methanol, and PS and nanoparticles were co-precipitated from the solution. After filtration and drying in vacuum at 60 °C for 5 days, the raw nanocomposites were obtained (cartoon of various PS nanocomposites is shown in **Scheme 2**). Finally, the raw nanocomposites were processed by compression molding at 190 °C for 5 minutes under a pressure of 10 MPa.

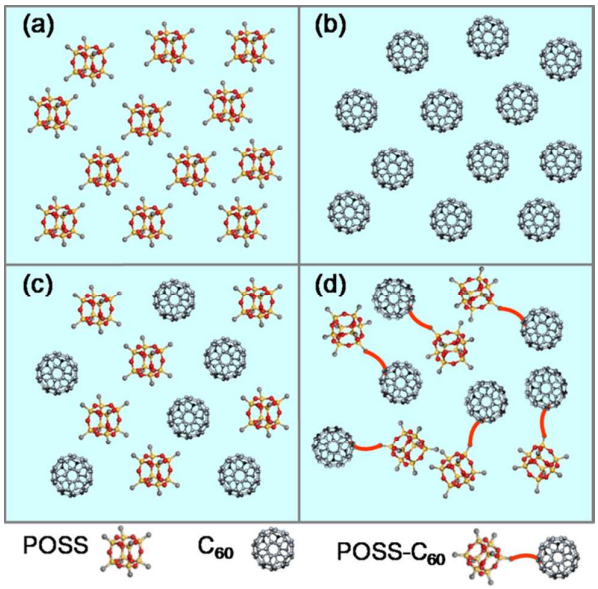

Scheme 2. Cartoon of (a)POSS, (b)C_{60}, (c)POSS/$C_{60}$and (d)POSS-C_{60} PS nanocomposites (the background colour represents PS).

2.4 Characterization

2.4.1 NMR, FT-IR and MALDI-TOF MS experiments. All NMR experiments were performed in $CDCl_3$ (J&K Chemicals, 99.8%) on a Bruker AV II-400 MHz NMR spectrometer. FT-IR spectrometer was obtained with a Nicolet 6700 spectrometer (Nicolet Instrument Company, USA). Matrix-assisted laser desorption/ionization time-of-flight (MALDI-TOF) mass spectra were recorded on a MALDITOF/TOF 5800 mass spectrometer (ABSciex, USA) with a positive reflection mode. The samples was prepared in $CHCl_3$ and trans-2-[3-(4-tert-buutylphenyl)-2-methyl-2-propenylidene]malonotitrile (DCTB, Aldrich, 99.9%) served as matrix at concentration of 20 mg/mL. Sodium triflate (NaTFA) was used as cationizing agent and was prepared in MeOH/$CHCl_3$ (v/v =1/3) at concentration of 5 mg/mL. Then matrix and NaTFA were mixed with the ratio of 10/1 (v/v).The sample preparation involved depositing 0.3 μL of matrix and salt mixture on the wells of a 384-well ground-steel plate, allowing the spots to dry, depositing 0.3 μL of each sample on a spot of dry matrix, and adding another 0.3 μL of matrix and salt mixture on top of the dry sample (sandwich method).[46] After evaporation of the solvent, the plate was inserted into the MALDI source. The attenuation of the laser was adjusted to minimize unwanted fragmentation and to maximize the sensitivity.

2.4.2 Scanning electron microscope (SEM). The morphologies of fracture surface of the nanocomposites were directly observed using a field emission-scanning electron microscope (FESEM) (Inspect F, FEI, USA) at 20 kV accelerating voltage. All specimens were sputter-coated with gold powder before examination.

2.4.3 Tensile properties. An Instron 4302 universal tensile testing machine was used to measure the tensile properties. The tensile specimens were cut from the compression-molded film with the width about 5 mm and the thickness about 0.4 mm. And the distance of two grips was 15 mm. A crosshead speed of 10 mm/min was applied to determine the tensile properties and the testing was performed at room temperature (22 °C).

2.4.4 Differential scanning calorimetry (DSC) measurement. The glass transition temperature (T_g) was studied using a TA Instruments differential scanning calorimetry (DSC) Q2000 with a Universal Analysis 2000 under nitrogen atmosphere. The around 4-5 mg specimens were cut from the compression-molded films. The samples were first heated from 40 °C to 180 °C at a rate of 20 °C/min, held for 3 min to erase any thermal history, cooled to 0 °C at 100 °C/min from the melt of the first scan. After held for 1 min, the second scan rate was 20 °C/min to 180 °C and the value of T_g was taken.

2.4.5 Thermogravimetric analysis (TGA). Thermogravimetric analysis (TGA) was performed on a thermo-analyzer instrument (TA Instruments Inc., USA) under a 40 mL/min flow of nitrogen gas at a scan rate of 20 °C/min from 40 to 600 °C. And the loaded samples were about 8-10 mg.

2.4.6 Rheological analysis. The melt rheological properties of nanocomposites were measured in a strain-controlled dynamic rheometer (Bohlin Gemini 2000, Malvern, British). Disk-like samples with diameters of 25 mm and thickness of 2 mm were used to test at 190 °C under nitrogen atmosphere to avoid thermo-oxidative degradation. And the strain amplitude was set as 1% and the frequency sweep was performed in the range of 0.01 to 100 Hz.

3. Results and Discussion

3.1 Characterization of BPOSS-MAL and POSS-C_{60}.

Recently, Cheng et al. prepared POSS-C_{60} dyad by Steglich esterification.[34] In that way, although the hydroxyl-

functionalized POSS was commercially available, the carboxylic acid functionalized C_{60} was difficult to synthesis at larger quantities. So it is necessary to develop a simple method to scale up the synthesis of POSS-C_{60}. To achieve this goal, a POSS malonate (BPOSS-MAL) was first prepared by condensation of BPOSS-NH_2 with ethyl hydrogen malonate. Then POSS-C_{60}could be conveniently synthesized using BPOSS-MAL and C_{60} via Bingel-Hirsch cyclopropanation under mild reaction conditions.

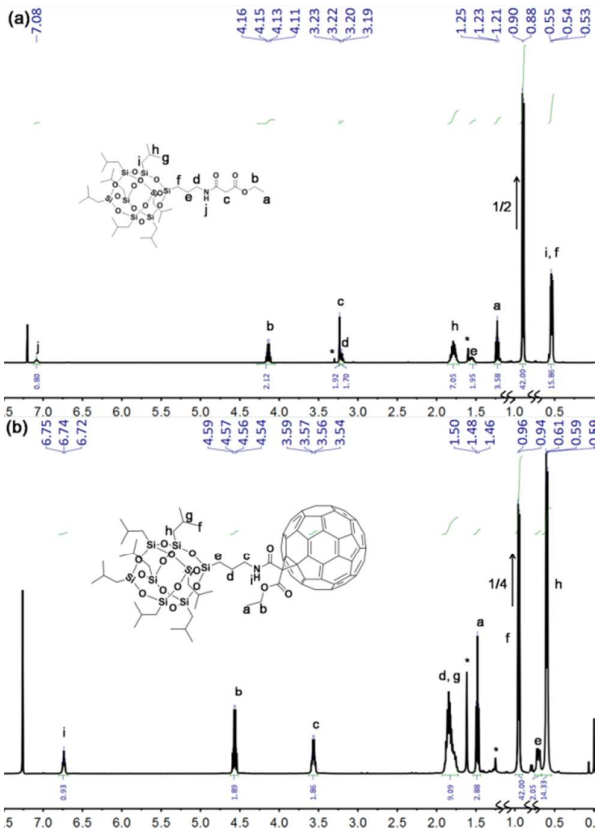

Figure. 1. The ^{1}H NMR of (a) BPOSS-MAL (*1 is residual solvent, *2 is water) and (b) POSS-C_{60} (*1 is water, *2 is grease).

In order to confirm the precise structure of BPOSS-MAL and POSS-C_{60}, ^{1}H NMR, ^{13}C NMR, MALDI-TOF mass spectra and FT-IR were used in this study. **Figure 1a** show the ^{1}H NMR results of BPOSS-MAL, the resonance atδ7.08 ppm assigned to the proton in amide group (-NHCO-). This prove that POSS-NH_2 and ethyl hydrogen malonate was condensation together. MALDI-TOF mass spectra (**Figure 2 a**), only one strong peak matching the proposed structure of BPOSS-MAL. The calculated monoisotopic mass for BPOSS-MAL ($C_{36}H_{77}NNaO_{15}Si_8$) is 1010.33 Da, which is very close to the observed m/z value of 1010.35 Da. For POSS-C_{60}, the protons (s, 2H, -$COCH_2CO_2$-) resonance at δ3.23ppm was disappeared and others protons can be found in the ^{1}H NMR spectra (**Figure 2 b**). MALDI-TOF mass spectra (**Figure 2 b**) further confirmed the structure of POSS-C_{60}. The calculated monoisotopic mass for POSS-C_{60} ($C_{96}H_{75}NNaO_{15}Si_8$) is 1728.32 Da, which is very close to the observed m/z value of 1728.42 Da. ^{13}C NMR (**Figure S1**) and FT-IR (**Figure S2**) also further confirmed the structure of BPOSS-MAL and POSS-C_{60}. In the ^{13}C NMR spectra, δ138.4-145.7 ppm assigned to the sp^2 hydird carbons in C_{60}. From FT-IR spectra, C_{60} peak at 526 cm^{-1} is also observed. And the detail data are summarized following the Synthetic procedures. In a word, we have successfully obtained dumbbell-shaped Janus POSS-C_{60} with high purity.

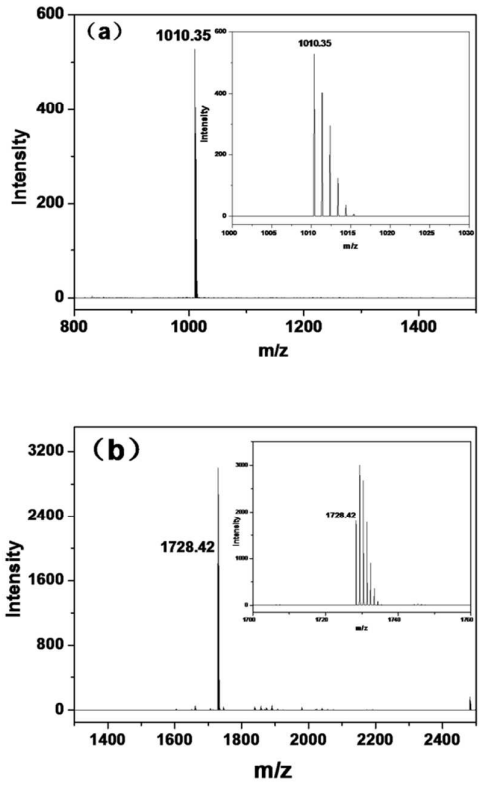

Figure. 2. The MALDI-TOF mass spectra of (a)BPOSS-MAL and (b)POSS-C_{60}.

3.2 Morphology and dispersion observation of PS nanocomposites.

It is well known that the dispersion of nanofillers in the polymer matrix plays a vital part in the physical properties of polymers, so the fracture surface morphology of nanocomposites was studied by SEM first. **Figure 3** shows the typical morphologies for the four kinds of typical samples, which are POSS-5, C_{60}-5, POSS/C_{60}-5 and POSS-C_{60}-5. It can be seen from **Figure 3** that POSS, C_{60}, POSS/C_{60} and POSS-C_{60} are randomly dispersed in the PS matrix. Even though the filler content is up to 5%, a fine dispersion of POSS was still achieved in the PS matrix. It is noteworthy that the diameter of POSS cage is around 1 nm and the C_{60} is 0.9 nm.[9, 13] The size of the aggregates is about 50-100 nm. As shown, the aggregates of POSS, C_{60}, POSS/C_{60} and POSS-C_{60} exist in PS matrix. This is probably because this kind of POSS is easily crystallisable.[47, 48] C_{60} also tends to form aggregates in polymer matrix[30] due to the strong and isotropic interactions between them.[49] However, the formation of 50-100 nm aggregates indicates that POSS, C_{60} and POSS-C_{60} have some compatibility with PS

matrix. So the solution-coagulation method provides a good way to make POSS, C_{60} and POSS-C_{60} disperse uniformly in PS. Thus the structure and properties of these four PS nanocomposites can be evaluated and compared.

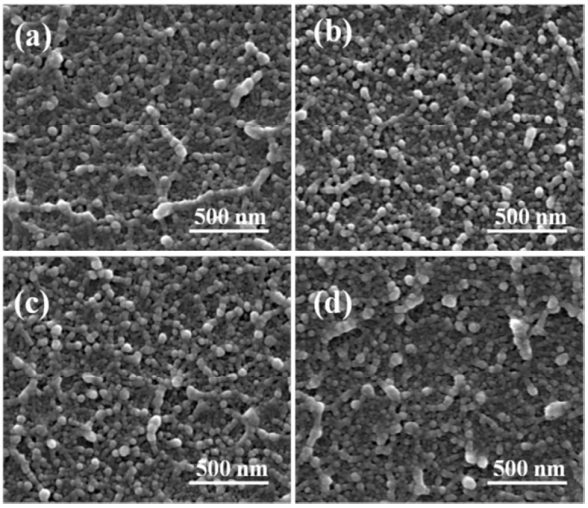

Figure. 3. Sectional SEM images showing an overall morphology of fracture surface for PS nanocomposites with 5 wt% of (a)POSS (b)C_{60} (c)POSS/C_{60} (d)POSS-C_{60}.

3.2 Tensile properties

The enhancement of mechanical properties of polymers has been strongly desired. We are always seeking for polymer nanocomposites that possess good mechanical properties. Blending nanofillers in polymer matrix is an effective way to enhance the strength of polymer. In this study, we investigated the effect of POSS, C_{60}, POSS/C_{60} and POSS-C_{60} on the PS strength. **Figure 4** shows the typical stress-strain curves of neat PS, PS/POSS, PS/C_{60}, PS/POSS/C_{60} and PS/POSS-C_{60}. And POSS, C_{60}, POSS/C_{60} and POSS-C_{60} have different effect on the tensile strength of PS which is shown in **Figure 5**. Although the overall enhancement for PS is limited, the variation trend is certain. With the increase of content of POSS, the fracture strength increases linearly. However, C_{60} plays an opposite role in the fracture strength of PS. Generally speaking, C_{60} decrease the fracture strength of PS at contents up to 5 wt%. For POSS/C_{60}, the fracture strength of PS increase when POSS/C_{60} is less than 1 wt%, but adding more POSS/C_{60}will decrease the fracture strength of PS. The effect of POSS/C_{60} for the fracture strength of PS is on the average of neat POSS and C_{60}, since only a half of POSS and C_{60} exist in the POSS/C_{60} physical blend. It has been report that POSS cage can cause significant effects for the improvement of mechanical properties.[50-53] Our results also suggest that with the increase of POSS loading above 1wt%, the fracture strength of PS increase. This also indicates a good compatibility between POSS and PS matrix. This behaviour is consistent with the increase of the interfacial area between POSS and PS matrix with the rise of the POSS concentration.[53] It is worth noting that the effect of POSS-C_{60} for fracture strength of PS is similar to POSS. And the results illustrate that POSS play a dominate role in the dumbbell-shaped JanusPOSS-C_{60} for the fracture strength of PS. From 0.5 to 5 wt%, the more POSS-C_{60} exist in PS, the greater fracture strength of PS. Considering the fact that only 50% of POSS exists in POSS-C_{60} nanoparticles, POSS-C_{60} shows the best enhancement in the four kinds of nanofillers even though POSS-C_{60} has a similar composition of "nano-atoms" with POSS/C_{60} physical blend.

It is well known that the dispersion of nanofillers in polymer matrix plays a key role in the physical properties of polymers. POSS-C_{60} is likely to form bi-layered structure.[34] The POSS we used in this work is easily crystallisable. C_{60} is more likely to aggregate within polymer matrix.[30] So they may aggregate and form different size to affect the mechanical properties of PS.

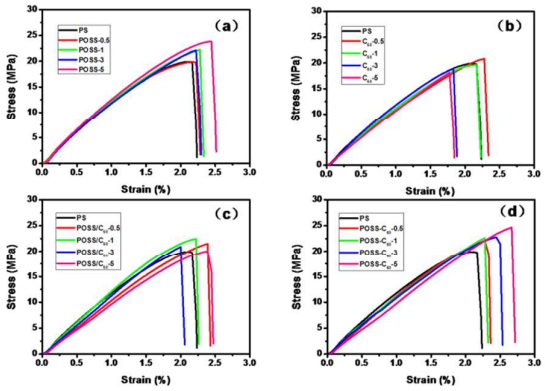

Figure. 4. Typical stress-strain curves of (a)PS/POSS, (b)PS/C_{60}, (c)PS/POSS/C_{60} and (d)PS/POSS-C_{60}.

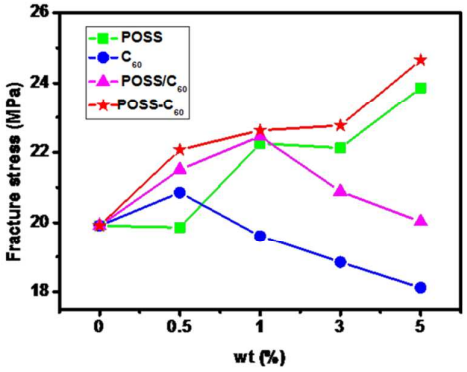

Figure. 5. The effect of various POSS, C_{60}, POSS/C_{60} and POSS-C_{60} loading on the fracture stress of PS nanocomposites.

3.3 Thermalproperties

C_{60} is known as a "radical sponge" since its 30 carbon-carbon double bonds are highly reactive toward free radicals.[54-56] So, C_{60} can theoretically trap the macromolecular or other radicals created from the pyrolisis of polymers and thus increasing the thermal stability of polymers.[29]

The thermal stability of these nanopaticles were first investigated. **Figure 6** presents the TGA curves of pristine POSS, C_{60}, POSS/C_{60} and POSS-C_{60} under nitrogen conditions. It

is obvious that pristine POSS begin to degrade rapidly at 220 °C and completely degraded at 310 °C. However, pristine C_{60} hardly degrade even at temperatures up to 600 °C. It is easy to imagine that POSS/C_{60} degrade at about 220 °C and show a platform from 310 to 600 °C. ButforPOSS-C_{60}, a slight mass loss occurs at about 205 °C, which is 15 °C lower than that of pristine POSS, and this mass loss can be attributed to the degradation of the ethyl hydrogen malonate on the cage surface of C_{60} during chemical reaction. And POSS-C_{60} degrade slower and have a better thermal stability than POSS/C_{60} physical blend until 600 °C. It is clear that the chemical linkage between POSS and C_{60} increases the thermal stability more effectively than simple physical blending. So we can draw a conclusion that there is a synergy between the two in POSS-C_{60}.

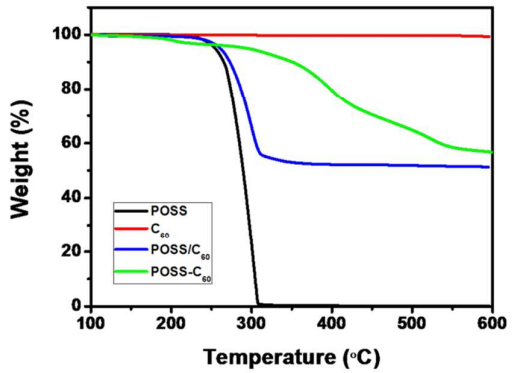

Figure. 6.TGA curves of pristine POSS, C_{60}, POSS/C_{60} and POSS-C_{60}under nitrogen conditions.

We also investigated the thermal stability of PS nanocomposites. As shown in **Figure 7**, with the addition of POSS from 0.5 to 5 wt%, the thermal stability of PS is almost unchanged. In contrast, loading C_{60} increases the thermal stability of PS even at concentrations as low as only 0.5 wt%. However, the addition of more C_{60} does not further improve the thermal stability of PS. The effect of POSS/C_{60} is on the average of neat POSS and C_{60}. Most notably is the change of PS/POSS-C_{60} nanocomposites. With the increasing weight percentage of POSS-C_{60}, the thermal stability of PS increases linearly and is different with POSS/C_{60} at the high nanoparticle loading. **Figure 8** gives the maximum weight loss temperature (T_{max}) data with various nanoparticle loading. By carefully comparing the results of PS/POSS, PS/C_{60}, PS/POSS/C_{60} and PS/POSS-C_{60}, we can find POSS-C_{60}-5 shows the highest T_{max} in all of the PS nanocomposites. And POSS-C_{60}-0.5, POSS-C_{60}-1, POSS-C_{60}-3 have a same effect with POSS/C_{60} for the PS nanocomposites.

The thermal stability of PS is enhanced when C_{60} exists in the PS nanocomposites, which may be due to the free-radical-trapping effect of C_{60}.[27] However, PS/POSS-C_{60}-5 shown the higher T_{max} than POSS/C_{60}-5 even C_{60}-5. It is worth noting that only a half of C_{60} exists in POSS-C_{60} comparing with pristine C_{60}. The possible reason is that POSS-C_{60} have different surface chemical structure, even they could form an alternating bi-layered structure when it is crystallization.[34] With the different aggregation structure, there are different surface contact area for the POSS-C_{60} with PS and the different ability to trap free radical is presented. So the thermal stability of POSS-C_{60}-5 is better than C_{60}-5.

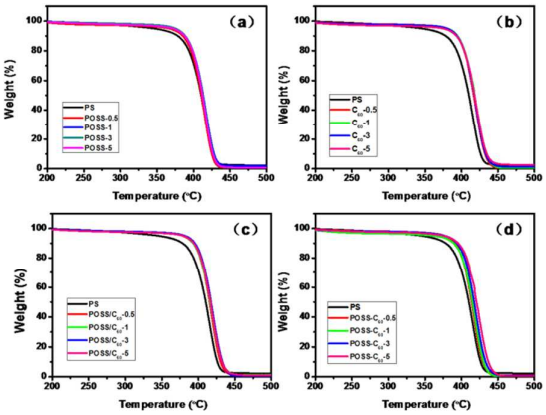

Figure. 7. TGA curves of PS nanocomposites under nitrogen conditions. (a) PS/POSS, (b) PS/C_{60}, (c) PS/POSS/C_{60} and (d) PS/POSS-C_{60}

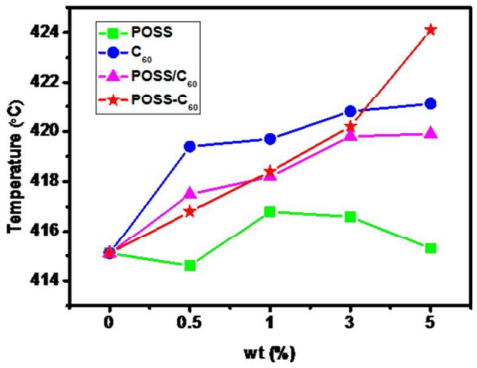

Figure. 8. The maximum weight loss temperature (T_{max}) data of PS/POSS, PS/C_{60}, PS/POSS/C_{60} and PS/POSS-C_{60} under nitrogen conditions.

3.4 Differential scanning calorimetry (DSC) measurement

Figure 9 shows the DSC thermograms of the nanocomposite at various loading of POSS, C_{60}, POSS/C_{60} and POSS-C_{60}. The neat PS has a T_g at 99.1 °C. When loading POSS in PS from 0.5 to 5 wt%, the PS/POSS shows an overall decrease of T_g. In PS/C_{60} nanocomposites, with the addition of more C_{60}, the T_g of PS nanocomposites becomes lower. Similar results were also found in PS/POSS/C_{60} nanocomposites. For POSS-C_{60}, the variation trend is also similar with POSS.

It is known that in blended systems the T_g strongly depends on the interaction of POSS with polymer and the method of blending.[11] The result is different with some studies which have a weaker increase of T_g.[57-59] However, there are also

some results similar with us.[60, 61] The effects of nanoparticles on T_g of polymer are complicated. Both POSS and C_{60} only have a weak interaction with PS. When nanoparticles are added, free volume develops around the nanoparticle and the effect finally displace of the weak interaction of nanoparticles with polymer chain segments. The chain mobility increases, resulting in a decrease of T_g. The POSS-C_{60} thus plays the role of a plasticizer.[61] In summary, the glass transition temperature (T_g) of PS is decreased as increasing the filler content in the similar way for the four kinds of PS nanocomposites.

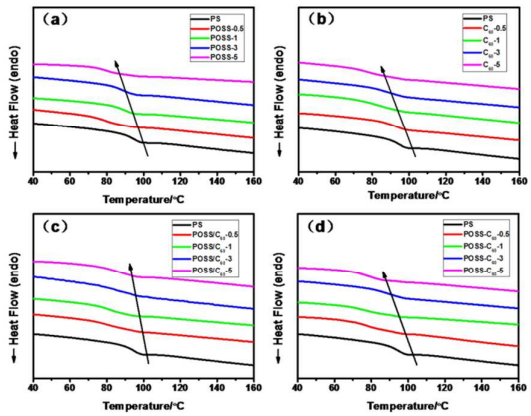

Figure. 9. DSC thermograms of PS nanocomposites. (a) PS/POSS, (b) PS/C_{60}, (c) PS/POSS/C_{60} and (d) PS/POSS-C_{60}.

3.5 Rheological analysis

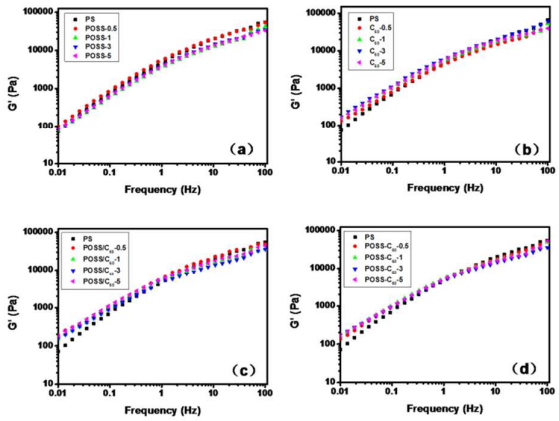

Figure.10. The dependence of storage moduli (G') of PS nanocomposites on frequency. (a)PS/POSS, (b)PS/C_{60}, (c)PS/POSS/C_{60} and (d)PS/POSS-C_{60}.

Owing to POSS and C_{60} have different surface chemical structure and energetic interactions, the POSS-C_{60}would form an alternating bi-layered structure by slow evaporation from dilute solution on various substrates in a solvent-saturated atmosphere.[34] So it is naturally to ask if POSS-C_{60} would form well-organized aggregate state structures in PS matrix. And how this structure affects the properties of PS nanocomposites. So PS nanocomposites were further studied using rheological measurement. **Figure 10** depicts the storage modulus (G'). From **Figure 10 a-d**, no obvious change happened in the storage modulus of PS at the frequencies from 0.01 to 100 Hz. The possible reasons are POSS (~1 nm), C_{60} (~1 nm), POSS-C_{60} (~3 nm) are too small, the low concentration of POSS-C_{60} and no polar functional group on the surface of them, so there is very little effect of POSS-C_{60} on PS nanocomposites. This further indicates that POSS, C_{60}, POSS/C_{60} and POSS-C_{60} have similar dispersion in PS matrix.

4. Conclusions

In this study, Bingel-Hirsch cyclopropanation was used to synthesize a dumbbell-shaped POSS-C_{60} at mild reaction conditions at gram-scale. This method provides a convenient way for the preparation of polymer/POSS-C_{60} nanocomposites. From a series of comparative experimental, we find that all of the nanofillers decrease the glass transition temperature (T_g) of PS and have little effect on the storage modulus (G') of PS. It is noteworthy that POSS-C_{60} exhibits a synergistic effect on the mechanical properties and thermal stability of PS. Interestingly, the POSS part of POSS-C_{60} plays a dominate role for the fracture strength of PS and the C_{60} part of POSS-C_{60} can increase the thermal stability of PS. In summary, our studies provides some idea for the design of new nanoparticles which could find good application even better "tailoring" the properties of polymer. In the future, we will design more MNP based on POSS and C_{60} with different functional group, and aim to improve the interface interaction with polymer matrix to prepare high performance polymer nanocomposites.

Acknowledgements

This work was supported by the National Natural Science Foundation of China (51421061 and 51210005).

Notes and references

1. J. C. Huang, *Advances in Polymer Technology*, 2002, **21**, 299-313.
2. M. Rong, M. Zhang and W. Ruan, *Materials science and technology*, 2006, **22**, 787-796.
3. R. Andrews and M. Weisenberger, *Current Opinion in Solid State and Materials Science*, 2004, **8**, 31-37.
4. Z. Jia, W. Yuan, H. Zhao, H. Hu and G. L. Baker, *RSC Advances*, 2014, **4**, 41087-41098.
5. L. Bi and J.-w. Wang, *Chinese Journal of Polymer Science*, 2013, **31**, 1546-1553.
6. S.-W. Kuo and F.-C. Chang, *Progress in Polymer Science*, 2011, **36**, 1649-1696.
7. I. Siró and D. Plackett, *Cellulose*, 2010, **17**, 459-494.
8. A. Pivrikas, N. Sariciftci, G. Juška and R. Österbacka, *Progress in Photovoltaics: Research and Applications*, 2007, **15**, 677-696.
9. R. H. Baney, M. Itoh, A. Sakakibara and T. Suzuki, *Chemical Reviews*, 1995, **95**, 1409-1430.
10. D. B. Cordes, P. D. Lickiss and F. Rataboul, *Chem. Rev*, 2010, **110**, 2081-2173.
11. K. N. Raftopoulos and K. Pielichowski, *Progress in Polymer*

Science, 2015.
12. F. Wang, X. Lu and C. He, *J Mater Chem*, 2011, **21**, 2775-2782.
13. H. W. Kroto, J. R. Heath, S. C. O'Brien, R. F. Curl and R. E. Smalley, *Nature*, 1985, **318**, 162-163.
14. W. Krätschmer, L. D. Lamb, K. Fostiropoulos and D. R. Huffman, *Nature*, 1990, **347**, 354-358.
15. K. M. Kadish and R. S. Ruoff, *Fullerenes: chemistry, physics, and technology*, John Wiley & Sons, 2000.
16. A. Hirsch and M. Brettreich, *Fullerenes: chemistry and reactions*, John Wiley & Sons, 2006.
17. Z. Zhang, A. Gu, G. Liang, P. Ren, J. Xie and X. Wang, *Polymer Degradation and Stability*, 2007, **92**, 1986-1993.
18. Y.-J. Lee, J.-M. Huang, S.-W. Kuo, J.-S. Lu and F.-C. Chang, *Polymer*, 2005, **46**, 173-181.
19. H. Brandhorst, T. Isaacs-Smith, B. Wells, J. D. Lichtenhan and B. X. Fu, 2006.
20. Y. Xue, Y. Liu, F. Lu, J. Qu, H. Chen and L. Dai, *The Journal of Physical Chemistry Letters*, 2012, **3**, 1607-1612.
21. J. M. Mabry, A. Vij, S. T. Iacono and B. D. Viers, *Angewandte Chemie*, 2008, **120**, 4205-4208.
22. A. Pan, S. Yang and L. He, *RSC Advances*, 2015, **5**, 55048-55058.
23. B. Zhang, Y. Chen, J. Wang, W. J. Blau, X. Zhuang and N. He, *Carbon*, 2010, **48**, 1738-1742.
24. J. Wu and P. T. Mather, 2009.
25. N. Sariciftci, L. Smilowitz, A. J. Heeger and F. Wudl, *Science*, 1992, **258**, 1474-1476.
26. B. C. Thompson and J. M. Frechet, *Angewandte chemie international edition*, 2008, **47**, 58-77.
27. P. Song, Y. Shen, B. Du, Z. Guo and Z. Fang, *Nanoscale*, 2009, **1**, 118-121.
28. P. a. Song, H. Liu, Y. Shen, B. Du, Z. Fang and Y. Wu, *Journal of Materials Chemistry*, 2009, **19**, 1305-1313.
29. P. Song, L. Zhao, Z. Cao and Z. Fang, *Journal of Materials Chemistry*, 2011, **21**, 7782-7788.
30. P. a. Song, Y. Zhu, L. Tong and Z. Fang, *Nanotechnology*, 2008, **19**, 225707.
31. W.-B. Zhang, X. Yu, C.-L. Wang, H.-J. Sun, I.-F. Hsieh, Y. Li, X.-H. Dong, K. Yue, R. Van Horn and S. Z. Cheng, *Macromolecules*, 2014, **47**, 1221-1239.
32. D. J. Clarke, J. G. Matisons, G. R. Simon, M. Samoc and A. Samoc, *Appl Organomet Chem*, 2008, **22**, 460-465.
33. D. J. Clarke, J. G. Matisons, G. P. Simon, M. Samoc and A. Samoc, *Appl Organomet Chem*, 2010, **24**, 184-188.
34. H.-J. Sun, Y. Tu, C.-L. Wang, R. M. Van Horn, C.-C. Tsai, M. J. Graham, B. Sun, B. Lotz, W.-B. Zhang and S. Z. Cheng, *Journal of Materials Chemistry*, 2011, **21**, 14240-14247.
35. M. Huang, C.-H. Hsu, J. Wang, S. Mei, X. Dong, Y. Li, M. Li, H. Liu, W. Zhang and T. Aida, *Science*, 2015, **348**, 424-428.
36. Z. Lin, P. Lu, C. H. Hsu, K. Yue, X. H. Dong, H. Liu, K. Guo, C. Wesdemiotis, W. B. Zhang and X. Yu, *Chem-Eur J*, 2014, **20**, 11630-11635.
37. F. Yang, C. Li, H. Guo, J. Ye and Z. Jiao, *Synthetic Communications*, 2012, **42**, 3664-3669.
38. A. Walther and A. H. Müller, *Soft Matter*, 2008, **4**, 663-668.
39. J. Hu, S. Zhou, Y. Sun, X. Fang and L. Wu, *Chemical Society Reviews*, 2012, **41**, 4356-4378.
40. A. Walther, K. Matussek and A. H. Muller, *Acs Nano*, 2008, **2**, 1167-1178.
41. R. Bahrami, T. I. Löbling, A. H. Gröschel, H. Schmalz, A. H. Müller and V. Altstädt, *ACS nano*, 2014, **8**, 10048-10056.
42. K. C. Bryson, T. I. Löbling, A. H. Müller, T. P. Russell and R. C. Hayward, *Macromolecules*, 2015.
43. W.-B. Zhang, Y. Tu, H.-J. Sun, K. Yue, X. Gong and S. Z. Cheng, *Science China Chemistry*, 2012, **55**, 749-754.
44. C. Bingel, *Chemische Berichte*, 1993, **126**, 1957-1959.
45. X. Camps and A. Hirsch, *Journal of the Chemical Society, Perkin Transactions 1*, 1997, 1595-1596.
46. Y. Li, W.-B. Zhang, J. E. Janoski, X. Li, X. Dong, C. Wesdemiotis, R. P. Quirk and S. Z. Cheng, *Macromolecules*, 2011, **44**, 3328-3337.
47. L. Liu, M. Tian, W. Zhang, L. Zhang and J. E. Mark, *Polymer*, 2007, **48**, 3201-3212.
48. H. Pan and Z. Qiu, *Macromolecules*, 2010, **43**, 1499-1506.
49. P. A. Heiney, J. E. Fischer, A. R. McGhie, W. J. Romanow, A. M. Denenstein, J. P. McCauley Jr, A. B. Smith and D. E. Cox, *Phys Rev Lett*, 1991, **66**, 2911.
50. C. Zhao, X. Yang, X. Wu, X. Liu, X. Wang and L. Lu, *Polymer Bulletin*, 2008, **60**, 495-505.
51. N. Hosaka, N. Torikai, H. Otsuka and A. Takahara, *Langmuir*, 2007, **23**, 902-907.
52. G. Pan, J. E. Mark and D. W. Schaefer, *Journal of Polymer Science Part B: Polymer Physics*, 2003, **41**, 3314-3323.
53. Y. Zhao and D. A. Schiraldi, *Polymer*, 2005, **46**, 11640-11647.
54. P. Krusic, E. Wasserman, P. Keizer, J. Morton and K. Preston, *Science*, 1991, **254**, 1183-1185.
55. L. Gan, S. Huang, X. Zhang, A. Zhang, B. Cheng, H. Cheng, X. Li and G. Shang, *Journal of the American Chemical Society*, 2002, **124**, 13384-13385.
56. T. Cao and S. Webber, *Macromolecules*, 1996, **29**, 3826-3830.
57. K. Tanaka, S. Adachi and Y. Chujo, *Journal of Polymer Science Part A: Polymer Chemistry*, 2009, **47**, 5690-5697.
58. S. Li, G. P. Simon and J. G. Matisons, *Polymer Engineering & Science*, 2010, **50**, 991-999.
59. J. H. Jeon, K. Tanaka and Y. Chujo, *Journal of Polymer Science Part A: Polymer Chemistry*, 2013, **51**, 3583-3589.
60. Y. Feng, Y. Jia, S. Guang and H. Xu, *J Appl Polym Sci*, 2010, **115**, 2212-2220.
61. J. Wu, T. S. Haddad and P. T. Mather, *Macromolecules*, 2009, **42**, 1142-1152.